

Bidirectional visible-NIR and biconical FT-IR reflectance spectra of Almahata Sitta meteorite samples

Takahiro HIROI^{1*}, Peter M. JENNISKENS², Janice L. BISHOP², Tahani S. M. SHATIR³,
Ayman M. KUDODA⁴, and Muawia H. SHADDAD⁴

¹Department of Geological Sciences, Brown University, Rhode Island 02912, USA

²SETI Institute, Carl Sagan Center, 515 N. Whisman Road, Mountain View, California 94043, USA

³University of Khartoum, P.O. Box 321-19, Khartoum 11115, Sudan

⁴Physics Department, Faculty of Science, University of Khartoum, P.O. Box 321, Khartoum 11115, Sudan

*Corresponding author. E-mail: Takahiro_Hiroi@brown.edu

(Received 25 December 2009; revision accepted 06 June 2010)

Abstract—Bidirectional visible and near-infrared and off-axis biconical FT-IR reflectance spectra of Almahata Sitta meteorite stone samples, fragments of asteroid 2008 TC₃, have been measured. These meteorites represent the first freshly fallen polymict ureilites available for such studies. Although the chip samples show varying degrees of terrestrial weathering depending on their environment on the Earth, many of them are much fresher than other ureilites known to date. The majority of the Almahata Sitta chips studied here show only a weak near-UV absorption, a flat spectrum at visible and near-IR wavelengths and varying depths of the 1 and 2 μm pyroxene and olivine bands. The astronomical reflectance observations of the asteroid 2008 TC₃ over the range 0.55–1.0 μm provide a constraint on what a combination of the measured spectra can represent in the surface reflectance of the asteroid over the 0.32–2.55 μm range measured in this study. Most of the recovered samples of Almahata Sitta have textures and albedos similar to stones #27 (largest recovered fragment), #4, and #47. Results of linear least-square fits of the asteroid 2008 TC₃ spectrum with two sets of the meteorite spectra suggest that the asteroid had 10–12% albedo and no fine regolith on its surface. We note that other lithologies may be at the surface of other fragments of the asteroid family from which 2008 TC₃ originated. In that case, reflectance spectra could vary significantly among family members.

INTRODUCTION

Almahata Sitta meteorite is the first observed fall from a tracked and spectrally observed asteroid, 2008 TC₃ (Jenniskens et al. 2009, 2010), which gave a rare opportunity to compare the observational data of an asteroid with those of the meteorites derived from it. Many of the Almahata Sitta stones are classified as polymict ureilite (e.g., Shaddad et al. 2010, ~~this issue~~), and most of them are very fresh and free from terrestrial weathering. Because almost all ureilite samples available to date have suffered varying degrees of terrestrial weathering (e.g., Cloutis and Hudon 2004; Cloutis et al. 2010), Almahata Sitta samples are also extremely useful for examining the effects of terrestrial weathering on ureilites.

Among many remote-sensing techniques, visible and near-infrared (VNIR) spectroscopy provides information mainly on silicate mineral composition of the remote surface and has been the primary technique for identifying meteorite parent bodies among asteroids (e.g., McCord et al. 1970; Gaffey et al. 1993; Pieters and McFadden 1994, Burbine 2000; Burbine et al. 2008). VNIR spectroscopy has also been shown to correlate well with mineralogy determined through petrology and other means for meteorites (e.g., Gaffey 1976; Sunshine et al. 1993; Bishop et al. 1998). Asteroids have been divided into classes based on their VNIR spectral properties (Bus and Binzel 2002; DeMeo et al. 2009) that enables comparison of these asteroid classes with meteorite types.

Taking advantage of this rare opportunity, a preliminary study of the VNIR reflectance spectra of

1 chip and powder samples of selected stones of the
 2 meteorite has been performed in order to give insights
 3 into the surface and internal compositions and possibly
 4 the surface physical properties of 2008 TC₃. In addition,
 5 Fourier transform infrared (FT-IR) reflectance spectra
 6 of the samples have been measured in order to
 7 investigate the degrees of terrestrial weathering and any
 8 trends of composition among the samples.

9 It is hoped that this preliminary study will provide
 10 hints on some important questions, such as (1) whether
 11 the reflectance spectra of meteorite samples collected
 12 from an asteroid can represent the observed surface
 13 reflectance spectrum of the asteroid, (2) what physical
 14 conditions on the asteroid surface could make them
 15 look different, and (3) whether the terrestrial weathering
 16 effects on the meteorite samples could significantly
 17 prevent solving such questions.

18 19 20 21 22 23 24 25 26 27 28 29 30 31 32 33 34 35 36 37 38 39 40 41 42 43 44 45 46 47 48 49 50 51 52 53 54

EXPERIMENTAL

The samples of the Almahata Sitta meteorite stones studied here are described in Table 1. Small (1–2 cm diameter) chip samples of 11 stones #4, #7, #19, #25, #27, #32, #36, #44, #47, #50, and #51 were each placed into a black dish embedded with aluminum foil oriented so that the freshest and flattest face was directed upward. Photos of the chip samples of stones #4 and #27 are shown in Fig. 1 as examples. An effort was made to scrape off the terrestrially weathered portions (identified by a rusty color) on each face with a needle. A portion of each of seven stone (#4, #19, #32, #36, #44, #50, and #51) chips were ground and dry-sieved into coarse (125–500 μm) and fine (<125 μm) particulate samples. A portion of the stone #47 chip was ground into a bulk powder <500 μm and separated into magnetic and nonmagnetic fractions using a standard hand-held magnet. The nonmagnetic fraction was further ground into a powder sample <75 μm because of its transparency and small quantity in order to improve the spectral measurements. Each powder sample was placed in a black Teflon dish that exhibits no spectral features in the wavelength region studied for spectral measurements.

Bidirectional visible and near-infrared (VNIR) reflectance spectra of the Almahata Sitta samples were measured using the RELAB Spectrometer (Pieters 1983; Pieters and Hiroi 2004) over the wavelength range from 320 to 2550 nm at 10 nm intervals. The sample surface area measured was a circular spot of about 3.5–9 mm in diameter depending on the sample size. All the chip and powder samples were measured at the standard viewing geometry of 30° incidence (*i*) and 0° emergence (*e*) angles with pressed Halon as the standard. Corrections were made for the absolute reflectance and absorption

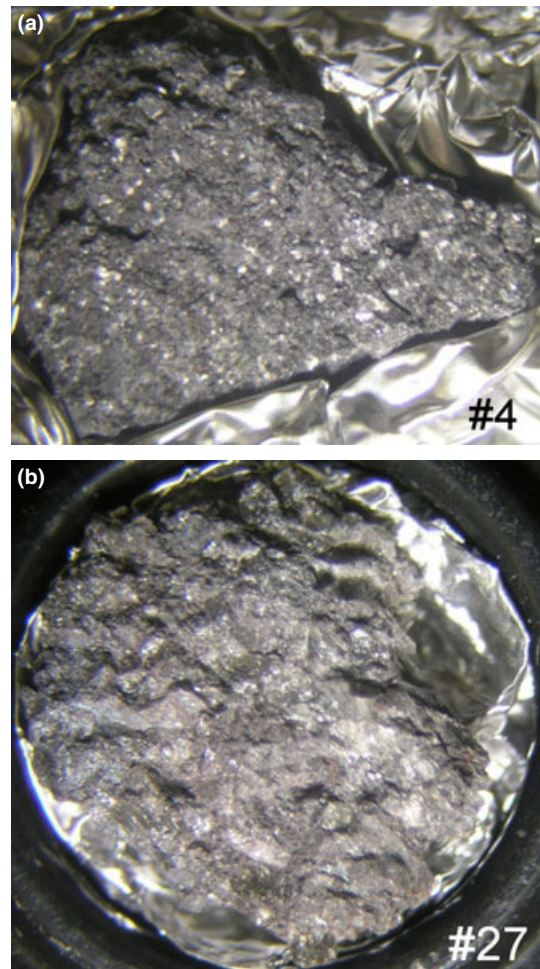


Fig. 1. Photos of chip samples of Almahata Sitta meteorite stones #4 and #27, embedded in aluminum foil for reflectance spectral measurements. The longest dimensions of the chips are about 1.4 and 1.0 cm, respectively.

features of Halon according to the standard RELAB procedure (Pieters 1983). In addition, five chip samples of stones #4, #7, #25, #27, and #47 were also measured at 19° *i* and 0° *e* with Spectralon as the standard to match the Sun-asteroid-Earth phase angle 18.6° for a spectral observation of the asteroid 2008 TC₃, from which these meteorite stones are presumed to be derived (Jenniskens et al. 2009). Each sample was spun at a rate of 1.5 s per rotation to average any heterogeneity over the azimuth angle. Corrections for the absorption bands of Halon and Spectralon were also made. Bidirectional VNIR spectra of chip samples of stones #19 and #32 embedded with black paper tape were also measured to ensure that there was no brightness increase due to the use of aluminum foil.

Off-axis biconical Fourier transform infrared (FT-IR) reflectance spectra of all the Almahata Sitta samples were measured over the wavelength range from

Table 1. Properties of Almahata Sitta meteorite stone samples analyzed.

No.	Texture	Mass (g)	Density (g cm ⁻³) ^a	Visible weathering	Reflectance (550 nm)
#4	Coarse grained	15	2.55 ± 0.08	None	0.097
#7	Fine grained, layered	1.5	–	None	0.156
#19	Fine grained	4.9	1.71 ± 0.20	Significant	0.156
#25	H5 chondrite clast	222	–	Some	–
#27	Coarse grained	284	2.83 ± 0.15	None	0.087
#32		130	2.98 ± 0.14		0.086
#36		58	2.67 ± 0.02		0.092
#44		2.3	–		0.108
#47	Coarse grained	54	2.94 ± 0.05	Severe ^b	0.110
#50		25	2.33 ± 0.17		0.075
#51		20	2.68 ± 0.06		0.087

^aShaddad et al. (2010), this issue.

^bFound in numerous small pieces.

7000 to 400 cm⁻¹ (about 1.4 to 25 μm in wavelength) with 4 cm⁻¹ resolution, using a Thermo Nexus 870 spectrometer, after they were purged in dry air overnight. The incident beam size on each sample was about 2–5 mm in diameter depending on the sample size. A diffuse gold surface was used as the reference standard.

Listed in Table 2 are RELAB IDs of the samples of which the reflectance spectra have been measured, and their spectral file names. These files will become downloadable from the RELAB website (<http://www.planetary.brown.edu/rehab/>) after a proprietary period of up to 3 yr.

RESULTS AND INTERPRETATIONS

VNR Spectra of Chip Samples

Bidirectional VNIR reflectance spectra of chip samples of stones #4, #7, #25, #27, and #47 of Almahata Sitta meteorite at two viewing geometries are shown in Fig. 2a. The spectral differences between the two viewing geometries are limited to slight variations in brightness and continuum slope, while still retaining the major absorption bands around 1 and 2 μm. The stone #4 chip has the weakest absorption features of the samples studied, whereas the #25, #27, #47 chips show dominant pyroxene bands around 1 and 2 μm, and the #7 chip shows a significant presence of an olivine component through a relatively strong 1.25 μm shoulder feature and a weak 2 μm band. The #27 and #4 stone chips have similar visible reflectance values to each other, which are also consistent with that of the asteroid 2008 TC₃ (Jenniskens et al. 2009).

The #25 chip is unique among all the chip samples measured in this study in that it shows very strong, well-defined absorption bands very similar to those of H chondrites (Jenniskens et al. 2010, this issue) and this meteorite has been classified in fact as an H5 chondrite

(Herrin et al. 2009). Microprobe analysis of iron oxide on this stone determined that the stone had fallen less than a few months prior (Zolensky et al. 2010, ~~this issue~~). ~~It was determined to have the same unusual PAH signature as other stones (Morrow et al. 2010, this issue)~~. In addition, the stone #25 was found among other ureilites of similar size (Shaddad et al. 2010, ~~this issue~~). These pieces of evidence suggest that this stone could have been a clast in the 2008 TC₃ asteroid (~~Morrow et al. 2010, this issue~~; Jenniskens et al. 2010, ~~this issue~~). Such clasts are not uncommon in ureilites.

Shown in Fig. 2b are the bidirectional VNIR reflectance spectra of chip samples of the remaining stones #19, #32, #36, #44, #50, and #51. A diversity of mineral compositions can be seen in these spectra, evident in the 1 μm absorption band shape. The three vertical broken lines in Fig. 2b indicate the approximate absorption band positions of olivine. The #32 and #44 chips show the strongest olivine signature, the #36, #50, and #51 chips show pyroxene-rich spectra with a significant 2 μm pyroxene band and little or no 1.25 μm olivine band, and the #19 chip shows an intermediate spectrum. Differences in the band centers near 1 and 2 μm in the stone #36, 50, and 51 spectra are attributed to differences in pyroxene composition, with longer wavelengths at each band being consistent with high-Ca pyroxene and shorter wavelengths with low-Ca pyroxene (Cloutis and Gaffey 1991; Sunshine and Pieters 1993), and/or the amount of coexisting olivine. An additional band between 0.85 and 0.9 μm in the stone #51 spectrum could be due to ferric oxides (e.g., Morris et al. 1985) from terrestrial weathering.

As an example of the effects of terrestrial weathering on the VNIR spectra, shown in Fig. 3 are the spectra of the weathered and fresh surfaces of stone #47 chip. The fresh surface of this stone #47 chip was a newly broken face. The weathered surface shows strong absorption in the UV range and an

Table 2. Reflectance experiment laboratory sample IDs and spectral file names of Almahata Sitta meteorite samples measured in this study. Viewing geometries for the bidirectional measurements are indicated as (incidence, emergence) angles in degrees.

Sample ID	Sample description	Bidirectional Vis-NIR		Biconical FT-IR
		(30, 0)	(19, 0)	
MT-PMJ-093	Stone #4 chip lighter face	C1MT93	C2MT93	BMR1MT093
MT-PMJ-093-B	Stone #4 125–500 μm	C1MT93B		BMR1MT093B
MT-PMJ-093-C	Stone #4 <125 μm	C1MT93C		BMR1MT093C
MT-PMJ-094	Stone #25 chip lighter face	C1MT94	C2MT94	BMR1MT094
MT-PMJ-095	Stone #7 chip lighter face	C1MT95	C2MT95	BMR1MT095
MT-PMJ-096	Stone #47 chip weathered face	C1MT96		BMR1MT096
MT-PMJ-097	Stone #27 chip lighter face	C1MT97	C2MT97	BMR1MT097
MT-PMJ-098	Stone #47 chip newly exposed fresher face	C1MT98	C2MT98	BMR1MT098
MT-PMJ-099	Stone #47 fresher powder <500 μm	C1MT99	C2MT99	BMR1MT099
MT-PMJ-100	Stone #47 weathered powder <500 μm	C1MT100		
MT-PMJ-101	Stone #47 fresher powder nonmagnetic <75 μm		C2MT101	BMR1MT101
MT-PMJ-102	Stone #47 fresher powder magnetic portion <500 μm		C2MT102	BMR1MT102
MT-PMJ-105	Stone #19 chip (embedded with Al foil or black tape)	C(1,2)MT105		BMR1MT105
MT-PMJ-105-A	Stone #19 chip (rust removed)	C1MT105A		BMR1MT105A
MT-PMJ-105-B	Stone #19 125–500 μm	C1MT105B		BMR1MT105B
MT-PMJ-105-C	Stone #19 <125 μm	C1MT105C		BMR1MT105C
MT-PMJ-106	Stone #32 chip (embedded with Al foil or black tape)	C(1,2)MT106		BMR1MT106
MT-PMJ-106-B	Stone #32 125–500 μm	C1MT106B		BMR1MT106B
MT-PMJ-106-C	Stone #32 <125 μm	C1MT106C		BMR1MT106C
MT-PMJ-107	Stone #36 chip	C1MT107		BMR1MT107
MT-PMJ-107-A	Stone #36 chip (rust removed)	C1MT107A		BMR1MT107A
MT-PMJ-107-B	Stone #36 125–500 μm	C1MT107B		BMR1MT107B
MT-PMJ-107-C	Stone #36 <125 μm	C1MT107C		BMR1MT107C
MT-PMJ-108	Stone #44 chip	C1MT108		BMR1MT108
MT-PMJ-108-A	Stone #44 chip (rust removed)	C1MT108A		BMR1MT108A
MT-PMJ-108-B	Stone #44 125–500 μm	C1MT108B		BMR1MT108B
MT-PMJ-108-C	Stone #44 <125 μm	C1MT108C		BMR1MT108C
MT-PMJ-109	Stone #50 chip	C1MT109		BMR1MT109
MT-PMJ-109-A	Stone #50 chip (rust removed)	C1MT109A		BMR1MT109A
MT-PMJ-109-B	Stone #50 125–500 μm	C1MT109B		BMR1MT109B
MT-PMJ-109-C	Stone #50 <125 μm	C1MT109C		BMR1MT109C
MT-PMJ-110	Stone #51 chip	C1MT110		BMR1MT110
MT-PMJ-110-A	Stone #51 chip (rust removed)	C1MT110A		BMR1MT110A
MT-PMJ-110-B	Stone #51 125–500 μm	C1MT110B		BMR1MT110B
MT-PMJ-110-C	Stone #51 <125 μm	C1MT110C		BMR1MT110C

absorption band at around 0.5 μm that are both typical of terrestrial weathering on metal-containing meteorite finds such as other urelites (Cloutis et al. 2010), primitive achondrites (Hiroi et al. 1993), and ordinary chondrites (Gooding 1981). The mafic signatures in spectra of other chip samples did not improve after attempts at removing the rusty-color portions from their surfaces.

VNIR Spectra of Powder Samples

Bidirectional reflectance spectra of such natural chip surfaces in general suffer from specularly reflecting surfaces which may suppress the mineral absorption band strengths, and the mineral assemblage exposed on

the measured surface may not necessarily represent the bulk average composition of the chip. Such a situation is depicted in Fig. 4a, wherein the bidirectional spectra of chip and powder samples of stone #4 are plotted. As the chip is ground into a coarse powder and then a fine powder, the absorption bands of olivine become clearer and clearer in this case. On the other hand, brightness decreases when the chip is ground into a coarse powder, and then increases again when ground into a fine powder. Increasing brightness is expected in general with decreasing particle size (e.g., Pieters 1983) and has been observed for spectra of olivines (e.g., Sunshine and Pieters 1998).

Shown in Fig. 4b are spectra of the bulk powder sample and magnetic and nonmagnetic portions of

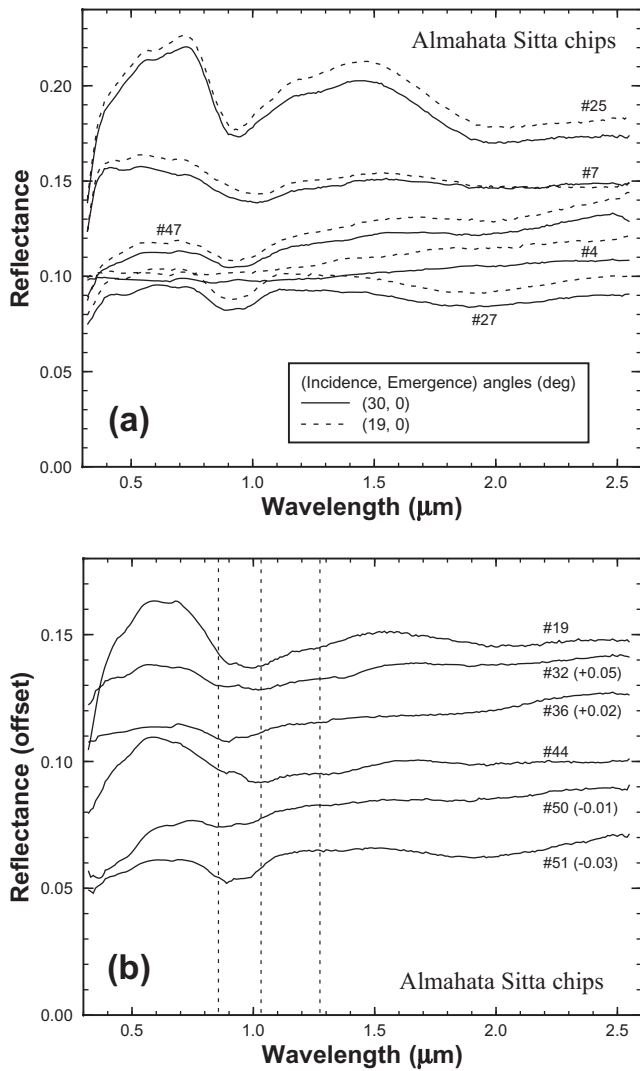


Fig. 2. Bidirectional visible and near-infrared (VNIR) reflectance spectra of Almahata Sitta meteorite chips. a) First group of chips measured both at the standard viewing geometry of 30° incidence and 0° emergence angles and at 19° incidence and 0° emergence angles to match the Sun-asteroid-Earth phase angle of a spectral observation of the asteroid 2008 TC₃. b) Second group of chips measured at the standard viewing geometry. Reflectance values are offset by the amounts indicated in parentheses after the stone numbers for clarity. Vertical broken lines indicate approximate wavelength positions of three absorption bands of olivine.

stone #47. The nonmagnetic portion shows a pyroxene-dominated spectrum, evident from its symmetric $1\ \mu\text{m}$ absorption band due to Fe^{2+} in the M2 site and $1.25\ \mu\text{m}$ shoulder band due to Fe^{2+} in the M1 site (e.g., Burns 1970; Pieters et al. 2005), with some terrestrial weathering evident from its $0.5\ \mu\text{m}$ absorption band. While the separation between metals and silicates does not seem perfect, these data clearly show a trend that this stone contains a significant amount of metallic iron

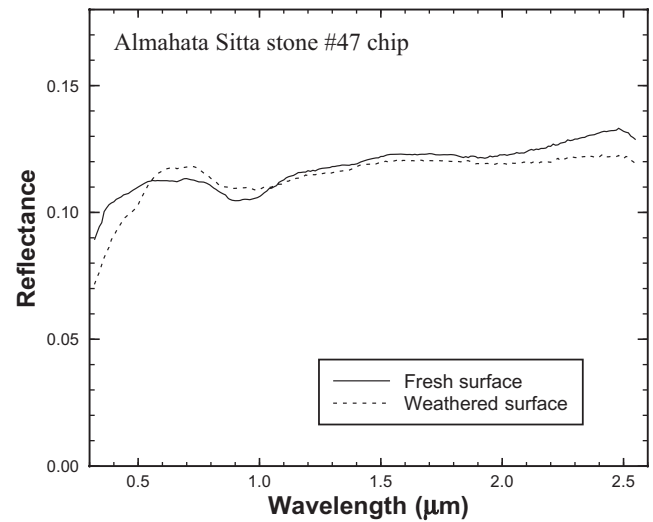


Fig. 3. Fresh and weathered surfaces of stone #47 chip measured at the standard viewing geometry.

as an agent (along with carbon) to cause the VNIR spectrum to become darker and reduce the strength of the absorption features.

Shown in Fig. 5 are the bidirectional VNIR spectra of (a) coarse and (b) fine powder samples of the same Almahata Sitta meteorite stones measured in Fig. 2b and stone #4 measured in Fig. 4. These spectra are plotted with offsets (indicated in the parentheses after the stone #) in the order of apparent mineral assemblage: olivine-rich at the top, and pyroxene-rich at the bottom. These powder samples have spectra that reflect their mineral composition more clearly than those of the chip samples plotted in Fig. 2. Spectra of the powder samples of stone #51 in Fig. 5 show relatively narrow absorption bands around 0.5 and $1.9\ \mu\text{m}$, which may be indicative of terrestrial weathering [ferric iron and structural water or hydroxyl absorption bands].

FT-IR Spectra of Powder Samples

Among the off-axis FT-IR spectra of the samples measured in this study, those of finely particulate samples are displayed as examples in Fig. 6 because of their better indication of mineral composition in this study than the spectra of stone surfaces. The spectra are offset and arranged in the same order as Fig. 5 in order to facilitate comparison of the spectra from both regions. Vertical broken lines around 8.4 and $16\ \mu\text{m}$ mark the Christiansen feature (Salisbury 1993) and a forsteritic olivine feature (Lane et al. 2009) that show a systematic variation indicating a compositional trend among these stones. The Christiansen feature around $8.4\ \mu\text{m}$ shifts toward the shorter wavelength and the

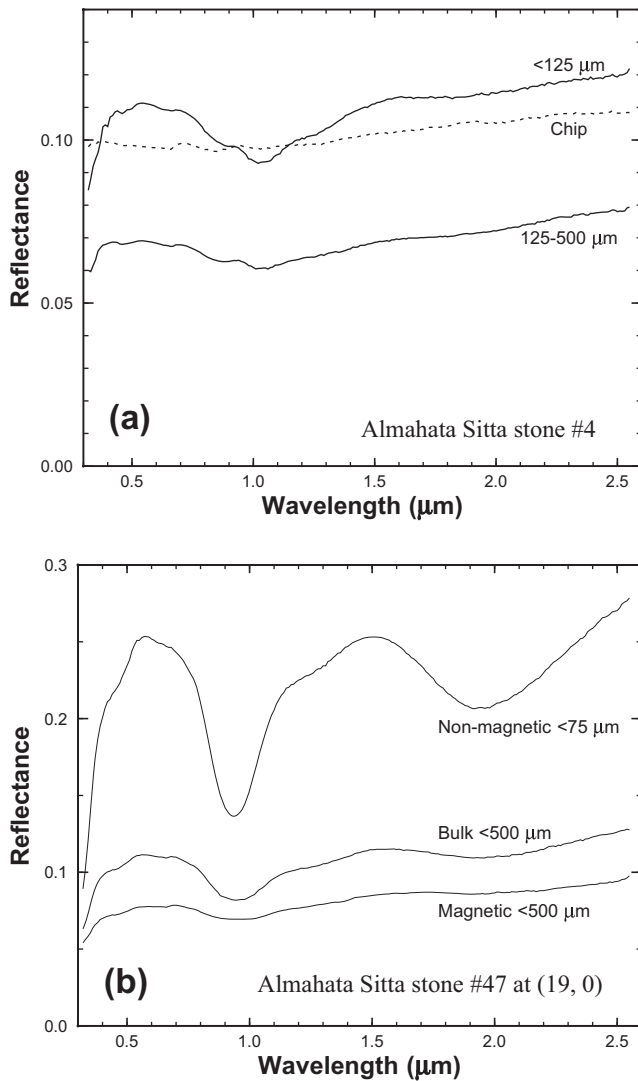


Fig. 4. Comparison of VNIR reflectance spectra of some samples of Almahata Sitta meteorite. a) Chip and powder samples of stone #4 measured at the standard viewing geometry. b) Bulk powder sample and magnetic and nonmagnetic portions of stone #47 measured at 19° incidence and 0° emergence angles.

positive reflectance peak around 16 μm becomes weaker as the pyroxene content increases. The #51 sample shows the strongest 3 μm water or hydroxyl band. In combination with the presence of the 0.5 and 1.9 μm bands in Fig. 5 as mentioned earlier, it is highly likely that the #51 stone spectra are affected by terrestrial weathering.

DISCUSSION

One notable aspect of the optical properties of the Almahata Sitta meteorite samples is the low reflectance

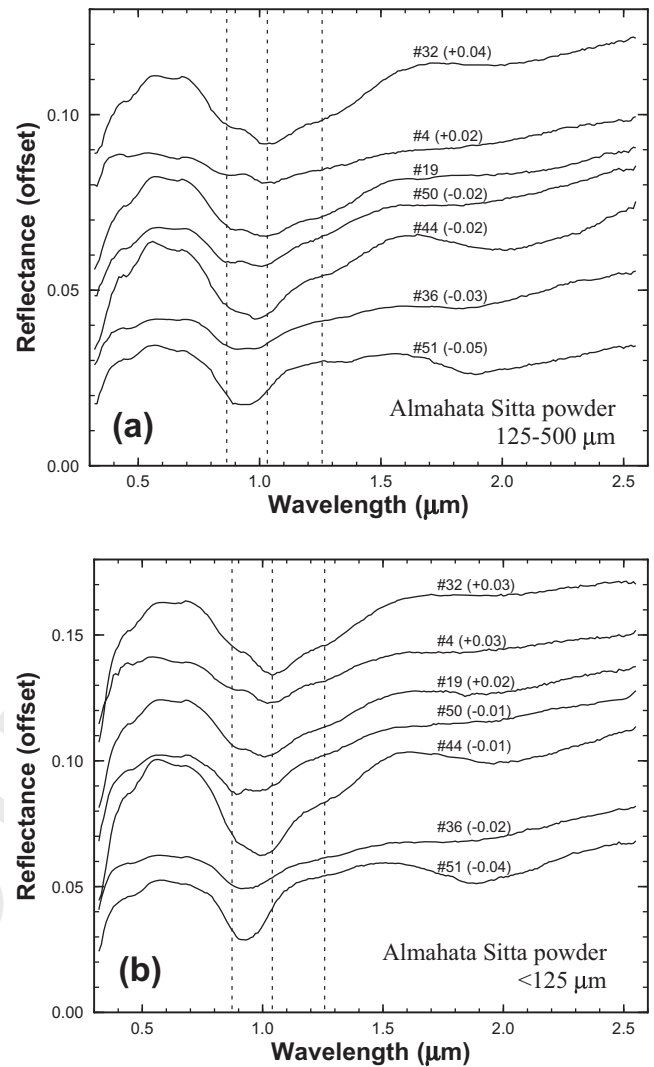


Fig. 5. Bidirectional VNIR reflectance spectra of (a) coarse powder samples (125–500 μm) and (b) fine powder samples (<125 μm) of Almahata Sitta meteorite measured at the standard viewing geometry. Reflectance values are offset by the amounts indicated in parentheses after the stone numbers for clarify. Vertical broken lines indicate approximate wavelength positions of three absorption bands of olivine.

of many of the stones, some of which are as dark as some carbonaceous chondrites. Ureilites in general contain both carbon and metallic iron as well as other opaques (e.g., Mittlefehldt et al. 1998), all of which contribute to their low reflectance. Because of presumed absence of organics as a darkening agent (Moroz et al. 1998) in ureilites, their darkening mechanism is expected to be simpler than that of carbonaceous chondrites. It is believed that differences of these Almahata Sitta meteorite stones in mineral grain size, carbon and/or metal content, and other accessory mineral composition contribute to their varying brightness. These samples

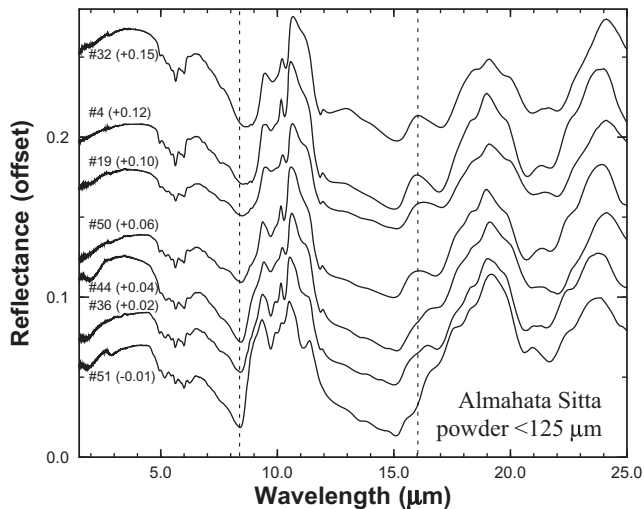


Fig. 6. Off-axis biconical Fourier-transform infrared (FT-IR) reflectance spectra of fine power samples (<125 μm) of Almahata Sitta meteorite. Reflectance values are offset by the amounts indicated in the parentheses for clarity. Indicated with broken lines are the Christiansen feature around 8.4 μm and another feature around 16 μm which may be indicative of compositional change.

are good materials provided by nature for studying the spectroscopic effects of mineral assemblage and texture.

The Surface Reflectance Spectrum of 2008 TC₃

Displayed in Figs. 7a and 7b are least-square fits of the observed extended visible reflectance spectrum of the asteroid 2008 TC₃ (Jenniskens et al. 2009) with linear combinations of the bidirectional spectra of two different sets of Almahata Sitta meteorite samples (1) Only the stone samples measured at 19° incidence and 0° emergence angles and (2) All the stone and powder samples measured at the standard viewing geometry. The asteroid albedo was also optimized for the best fit (about 0.12 and 0.10, respectively). Both cases produce the relatively flat visible spectrum and weak near-UV and 1 μm band absorptions similar to that of the asteroid, as well as weak 1.25 and 2 μm absorption bands. The latter case contains chip samples and only the coarse powder sample of stone #4 among powder samples. These results suggest that asteroid 2008 TC₃ had a visible reflectance of about 0.11 and no fine regolith on its surface, and would have shown a weak 2 μm absorption band if the NIR spectrum had been measured.

This reflectance estimate is more than twice the value of 0.046 ± 0.005 reported by Jenniskens et al. (2009). The latter value was measured at 19° incidence angle on dark parts of stone #7 sample, which contained several pyroxene rich white spots (see figure

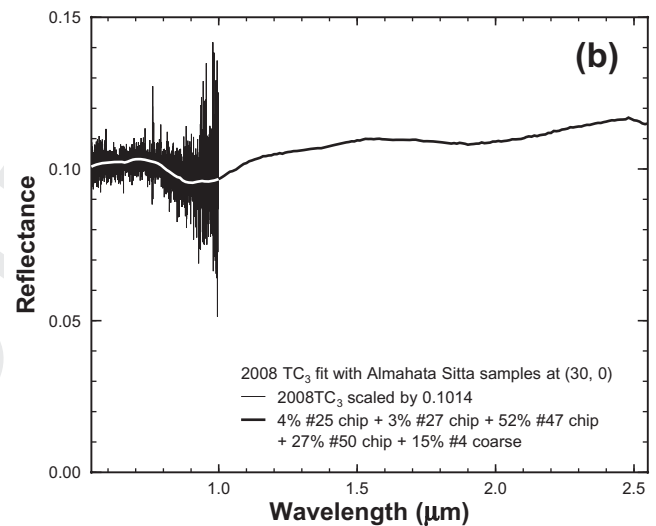
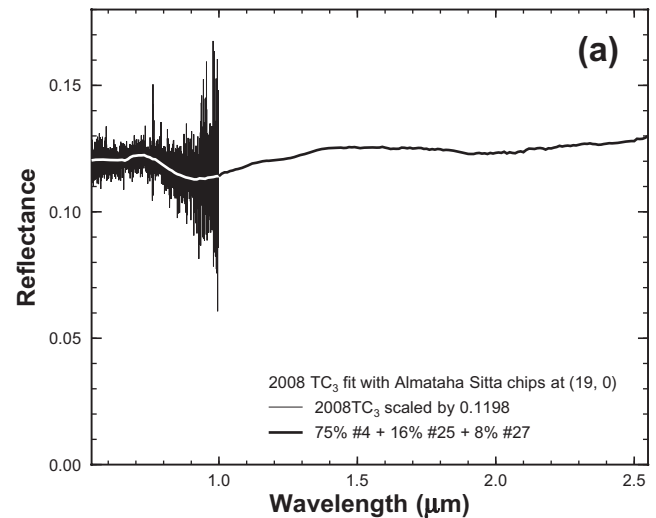


Fig. 7. Linear least-square fits of the observed reflectance spectrum of asteroid 2008 TC₃ (courtesy of Alan Fitzsimmons) with the VNIR spectra of two different sets of Almahata Sitta meteorite samples: a) chip samples measured at 19° incidence and 0° emergence angles (Fig. 2a), and b) chip and powder samples measured at the standard viewing geometry (Figs. 2 and 5). The asteroid reflectance spectrum was scaled up or down for the best match with the combined laboratory spectra.

in Jenniskens et al. 2009). The mean surface reflectance of #7 was measured at 0.089. Data were collected against an Ocean Optics diffuse reflectance standard WS-1 (made of PTFE plastic). We repeated the measurement of sample #7 against a Halon standard and obtained a visible reflectance of 0.157 (Fig. 2a), nearly a factor of two higher, but the spectral shape remained in good agreement with Jenniskens et al. (2009).

We were not able to account for the factor of two difference. The Ocean Optics reflectance standard was

1 measured against the Halon standard used here, and
 2 found to raise the earlier reported reflectance values by
 3 only 2% (reflectance = 0.047). The effect of possible
 4 light scattering from the background aluminum foil was
 5 verified by repeating the measurements for samples #19
 6 and #32 with a black tape background. This resulted in
 7 an increase of reflectance values by 2%, well within the
 8 range of uncertainty. The Halon standard was
 9 compared to 99%, 40%, 20%, and 10% reflectance
 10 standards from Labsphere, showing good linearity in
 11 the reflectance scale with an offset of -0.030 ± 0.005
 12 in the ratio of the Labsphere standards against Halon.
 13 Because the Labsphere reflectance standards were
 14 measured in a different viewing geometry (directional-
 15 hemispherical) from that of RELAB, these differences
 16 cannot simply be instrumental. If the measured
 17 reflectance values of the Almahata Sitta chip samples
 18 are corrected by this value (+0.03), their differences
 19 from that of asteroid 2008 TC₃ would increase.

21 The Range of Manifestations of Ureilite Parent Bodies

22
 23 It is challenging to postulate the spectral character
 24 of the asteroid parent body from spectra of its
 25 meteorites; however, analysis of multiple stone surfaces
 26 and particulate samples and consideration of the effects
 27 of space weathering and surface regolith provide
 28 constraints on the spectra of the parent body. The
 29 variations in spectral properties of the Almahata Sitta
 30 meteorites suggest that other asteroids from the asteroid
 31 family of which 2008 TC₃ originated may show other
 32 lithologies such as pyroxene-rich stone #51 on the
 33 surface and thus produce a different reflectance
 34 spectrum. Therefore, that asteroid family is expected to
 35 have member asteroids with a variety of reflectance
 36 spectra.

37 Scattering by surface regolith on larger bodies than
 38 2008 TC₃ could make the reflectance spectrum of a
 39 parent body resemble more closely that of the Almahata
 40 Sitta powder samples. While the Almahata Sitta chips
 41 are characterized by dark and flat spectra most
 42 consistent with F-class and possibly C-class asteroid
 43 spectra (DeMeo et al. 2009; Jenniskens et al. 2009),
 44 the particulate spectra are not as dark and exhibit stronger
 45 silicate mineral features. The olivine and pyroxene
 46 bands, uncommon in C-class asteroid spectra, are not
 47 unlike that of S-class asteroid spectra. A preliminary
 48 comparison of selected Almahata Sitta particulate
 49 spectra with S-type asteroid spectra is presented in
 50 Fig. 8. The systematic reddening trend of asteroid
 51 spectra, especially below about 0.7 μm in wavelength,
 52 is due to space weathering, which cannot be compared
 53 with the meteorite spectra. Based on the mineral
 54 absorption bands alone, parent bodies of ureilites

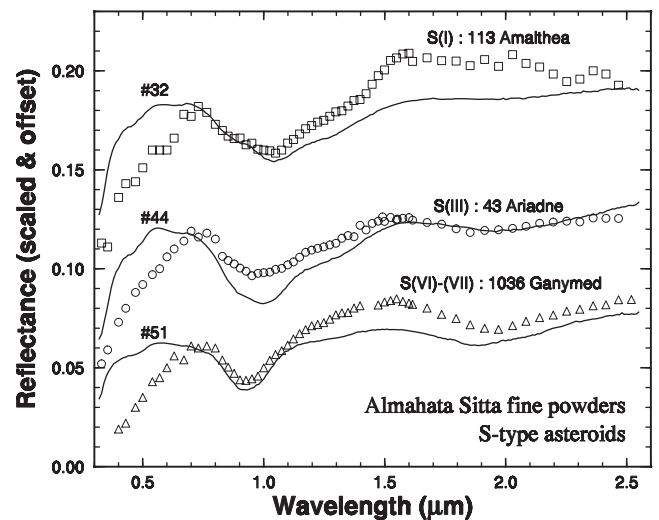


Fig. 8. Comparison of the VNR spectra of fine powder samples of some Almahata Sitta meteorite stones and S-type asteroids (Chapman and Gaffey 1979; Bell et al. 1988).

similar to Almahata Sitta may be hidden among olivine-rich A- or S(I)-class asteroids showing spectra similar to #32 powders in Fig. 5 (plus space weathering), or among other S- or Q-class asteroids showing varying olivine-pyroxene ratios in their spectra similar to #44, #36, and #51 in Fig. 5. The fact that such is not the case of asteroid 2008 TC₃ suggests that its surface is not covered with fine regolith or space weathered in the same manner as the A- or S-class asteroid surfaces are.

The spectral effects of space weathering on ureilites are unknown, but studies on carbonaceous chondrites indicate that space weathering can alter the spectral brightness, continuum slope, and the apparent strength of silicate absorption features (e.g., Hiroi et al. 2004; Moroz et al. 2004). The effects of space weathering appear also to be dependent on the abundance of organics in the matrix (Lazzarin et al. 2006) and more studies are needed to quantify these effects. If the visible continuum slope is sufficiently changed, independent of the near-IR slope, then other parent bodies of ureilites similar to the Almahata Sitta meteorite could spectrally appear as A, C, S, or Q class, other than the F class originally attributed to the asteroid 2008 TC₃, depending on which lithology among the stones studied here exists on the surface and the degree of space weathering that occurred. Laboratory studies of space weathering on fresh ureilite samples are needed to investigate the influence of this process for ureilites.

CONCLUSIONS

Almahata Sitta meteorite stones studied here show a diversity of mineral compositions based on reflectance

1 spectroscopy. All spectra exhibit low reflectance
 2 consistent with the presence of fine-grained opaques
 3 and/or metal. A mix of chip and coarse powder samples
 4 of stones #27, #4, and #47 may represent the surface
 5 composition of the asteroid 2008 TC₃ when it was
 6 spectrally observed, while other lithologies may
 7 represent its interior. A range of possible spectral
 8 shapes in the near-UV and near-IR range was presented
 9 including spectra of some stones having features
 10 characteristic of pyroxene and others characteristic of
 11 olivine. Spectral comparisons of various meteorite chip
 12 and particulate samples suggested that the asteroid 2008
 13 TC₃ did not have a fine-grained regolith or S-type space
 14 weathering on its surface. Other parent bodies of
 15 ureilites similar to the Almahata Sitta meteorite could
 16 spectrally appear as other classes than the F class
 17 originally attributed to the asteroid 2008 TC₃,
 18 depending on which lithology among the stones studied
 19 here existed on the surface and the degree of space
 20 weathering that occurred.

21
 22 *Acknowledgments*—We thank the students and staff of
 23 the University of Khartoum for their efforts in
 24 recovering the meteorites and making samples available
 25 for study. Reflectance spectra of all the samples in this
 26 study were measured at the NASA/Keck reflectance
 27 experiment laboratory (RELAB), Brown University, a
 28 multiuser facility supported by NASA Planetary
 29 Geology and Geophysics grant NNG06GJ31G. PJ is
 30 supported by a grant from the Planetary Astronomy
 31 program. We also appreciate Drs. Lucy McFadden,
 32 Tim McCoy, and Ed Cloutis for their helpful reviews.

33
 34 *Editorial Handling*—Dr. Beth Ellen Clark

35 REFERENCES

- 36
 37
 38 Bell J. F., Owensby P. D., Hawke B. R., and Gaffey M. J.
 39 1988. The 52-color asteroid survey: Final results and
 40 interpretation (abstract). 19th Lunar and Planetary Science
 41 Conference. p. 57.
- 42 Bishop J. L., Mustard J. F., Pieters C. M., and Hiroi T. 1998.
 43 Recognition of minor constituents in reflectance spectra of
 44 ALH 84001 chips and the importance for remote sensing
 45 on Mars. *Meteoritics & Planetary Science* 33:693–698.
- 46 **1** Burbine T. H. 2000. Forging asteroid-meteorite relationships
 47 through reflectance spectroscopy. Ph.D. thesis,
 48 Massachusetts Institute of Technology.
- 49 Burbine T. H., Rivkin A. S., Noble S. K., Mothé-Diniz T.,
 50 Bottke W. F., McCoy T. J., Dyar M. D., and Thomas C.
 51 A. 2008. Oxygen and asteroids. *Reviews in Mineralogy and*
 52 *Geochemistry* 68:273–343.
- 53 Burns R. G. 1970. *Mineralogical applications of crystal-field*
 54 *theory*. Cambridge, UK: Cambridge University Press.
- 55 Bus S. J. and Binzel R. P. 2002. Phase II of the small main-
 belt asteroid spectroscopic survey, a feature-based
 taxonomy. *Icarus* 158:146–177.
- Chapman C. R. and Gaffey M. J. 1979. Reflectance spectra for
 277 asteroids. In *Asteroids*, edited by Gehrels T. Tucson,
 AZ: The University of Arizona Press. pp. 655–687.
- Cloutis E. A. and Gaffey M. J. 1991. Pyroxene spectroscopy
 revisited: Spectral-compositional correlations and
 relationships to geothermometry. *Journal of Geophysical*
Research 96:22809–22826.
- Cloutis E. A. and Hudon P. 2004. Reflectance spectra of
 ureilites: Nature of the mafic silicate absorption features
 (abstract #1257). 35th Lunar and Planetary Science
 Conference. CD-ROM.
- Cloutis E. A., Hudon P., Romanek C. S., Reddy V., Gaffey M.
 J., and Hardersen P. S. 2010. Spectral reflectance properties
 of ureilites. *Meteoritics & Planetary Science* (submitted). **3**
- DeMeo F. E., Binzel R. P., Slivan S. M., and Bus S. J. 2009.
 An extension of the Bus asteroid taxonomy into the near-
 infrared. *Icarus* 202:160–180.
- Gaffey M. J. 1976. Spectral reflectance characteristics of the
 meteorite classes. *Journal of Geophysical Research* 81:905–
 920.
- Gaffey M. J., Bell J. F., Brown R. H., Burbine T. H., Piatek
 J. L., Reed K. L., and Chaky D. A. 1993. Mineralogical
 variations within the S-type asteroid class. *Icarus* 106:573–
 602.
- Gooding J. L. 1981. Mineralogical aspects of terrestrial
 weathering effects in chondrites from Allan Hills,
 Antarctica. Proceedings, 12B Lunar and Planetary Science
 Conference. pp. 1105–1122.
- Herrin J. S., Le L., Zolensky M. E., Ito M., Jenniskens P.,
 and Shaddad M. H. 2009. Late reduction texture in
 Almahata Sitta ureilite (abstract #9.07). DPS meeting #41.
 American Astronomical Society.
- Hiroi T., Bell J. F., Takeda H., and Pieters C. M. 1993.
 Modeling of S-type asteroid spectra using primitive
 achondrites and iron meteorites. *Icarus* 102:107–116.
- Hiroi T., Pieters C. M., Rutherford M. J., Zolensky M. E.,
 Sasaki S., Ueda Y., and Miyamoto M. 2004. What are the
 P-type asteroids made of? (abstract #1616). 35th Lunar
 and Planetary Science Conference. CD-ROM.
- Jenniskens P., Shaddad M. H., Numan D., Elsir S., Kudoda
 A. M., Zolensky M. E., Le L., Robinson G. A., Friedrich
 J. M., Rumble D., Steele A., Chesley S. R., Fitzsimmons
 A., Duddy S., Hsieh H. H., Ramsay G., Brown P. G.,
 Edwards W. N., Tagliaferri E., Boslough M. B., Spalding
 R. E., Dantowitz R., Kozubal M., Pravec P., Borovicka J.,
 Charvat Z., Vaubaillon J., Kuiper J., Albers J., Bishop J.
 L., Mancinelli R. L., Sandford S. A., Milam S. N., Nuevo
 M., and Worden S. P. 2009. The impact and recovery of
 asteroid 2008 TC₃. *Nature* 458:485–488.
- Jenniskens P., Vaubaillon J., Binzel R. P., DeMeo F. E.,
 Nesvorný D., Fitzsimmons A., Hiroi T., Marchis F.,
 Bishop J. L., Zolensky M. E., Herrin J. S., and Shaddad
 M. H. 2010. 2008 TC₃ and the search for the ureilite
 parent body. *Meteoritics & Planetary Science* 45. This
 issue.
- Lane M. D., Glotch T. D., Dyar M. D., Pieters C. M., Klima
 R., Hiroi T., Bishop J. L., and Sunshine J. M. 2009.
Midinfrared multi-technique spectroscopy of synthetic
olivines (forsterite to fayalite). San Francisco, CA: AGU
 Fall Meeting. **4**
- Lazzarin M., Marchi S., Moroz L. V., Brunetto R., Magrin
 S., Paolicchi P., and Strazzulla G. 2006. Space weathering
 in the main asteroid belt: The big picture. *The*
Astrophysical Journal 647:179–182.

- 1 McCord T. B., Adams J. B., and Johnson T. V. 1970.
2 Asteroid Vesta: Spectral reflectivity and compositional
3 implications. *Science* 168:1445–1447.
- 4 Mittlefehldt D. W., McCoy T. J., Goodrich C. A., and
5 Kracher A. 1998. Non-chondritic meteorite from asteroidal
6 **5** bodies. In *Planetary materials*, edited by Papike J. J.,
7 *Reviews in Mineralogy* 36, chap. 4. pp. 73–95.
- 8 Moroz L. V., Arnold G., Korochantsev A. V., and Wäsch R.
9 1998. Natural solid bitumens as possible analogs for
10 cometary and asteroid organics: 1. Reflectance
11 spectroscopy of pure bitumens. *Icarus* 134:253–268.
- 12 Moroz L. V., Baratta G., Atrazzulla G., Starukhina L., Dotto
13 E., Barucci M. A., Arnold G., and Distefano E. 2004.
14 Optical alteration of complex organics induced by ion
15 irradiation: 1. Laboratory experiments suggest unusual
16 space weathering trend. *Icarus* 170:214–228.
- 17 Morris R. V., Lauer H. V. Jr., Lawson C. A., Gibson E. K.
18 Jr., Nace G. A., and Stewart C. 1985. Spectral and
19 other physicochemical properties of submicron powders
20 of hematite (a-Fe₂O₃), maghemite (g-Fe₂O₃), magnetite
21 (Fe₃O₄), goethite (a-FeOOH), and lepidocrocite
22 (g-FeOOH). *Journal of Geophysical Research* 90:3126–
23 3144.
- 24 ~~Morrow et al. 2010. *Meteoritics & Planetary Science* 45. This
25 issue.~~
- 26 **6** Pieters C. M. 1983. Strength of mineral absorption features in
27 the transmitted component of near-infrared reflected
28 light—First results from RELAB. *Journal of Geophysical
29 Research* 88:9534–9544.
- 30 Pieters C. M. and Hiroi T. 2004. RELAB (Reflectance
31 Experiment Laboratory): A NASA multiuser spectroscopy
32 facility (abstract #1720). 35th Lunar and Planetary Science
33 Conference. CD-ROM.
- 34 Pieters C. M. and McFadden L. A. 1994. Meteorite and
35 asteroid reflectance spectroscopy: Clues to early solar
36 system processes. *Annual Review of Earth and Planetary
37 Sciences* 22:457–497.
- 38 Pieters C. M., Binzel R. P., Bogard D., Hiroi T., Mittlefehldt D.
39 W., Nyquist L., Rivkin A., and Takeda H. 2005. Asteroid-
40 meteorite links: The Vesta conundrum(s). *Proceedings of the
41 International Astronomical Union* 1:273–288.
- 42 Salisbury J. W. 1993. Mid-infrared spectroscopy: Laboratory
43 data. In *Remote geochemical analysis: Elemental and
44 mineralogical composition*, edited by Pieters C. M. and
45 Englert P. A. J. Cambridge, UK: Cambridge University
46 Press. pp. 79–98.
- 47 Shaddad M. H., Jenniskens P. M., Kudoda A. M., Numan
48 D., Elsir S., Riyad I. F., Ali A. E., Alameen M., Alameen
49 N. M., Eid O., Osman A. T., AbuBaker M. I., Chesley S.
50 R., Chodas P. W., Albers J., Edwards W. N., Brown P.
51 G., Kuiper J., and Friedrich J. M. 2010. The recovery of
52 asteroid 2008 TC₃. *Meteoritics & Planetary Science* 45.
53 This issue.
- 54 Sunshine J. M. and Pieters C. M. 1993. Estimating modal
55 abundances from the spectra of natural and laboratory
56 pyroxene mixtures using the Modified Gaussian Model.
57 *Journal of Geophysical Research* 98:9075–9087.
- 58 Sunshine J. M. and Pieters C. M. 1998. Determining the
59 composition of olivine from reflectance spectroscopy.
60 *Journal of Geophysical Research* 103:13,675–13,688.
- 61 Sunshine J. M., McFadden L. A., and Pieters C. M. 1993.
62 Reflectance spectra of the Elephant Moraine A79001
63 meteorite: Implications for remote sensing of planetary
64 bodies. *Icarus* 105:79–91.
- 65 Zolensky ~~et al.~~ 2010. *Meteoritics & Planetary Science* 45. This
66 issue. **7**

Author Query Form

Journal: MAPS

Article: 1097-1278

Dear Author,

During the copy-editing of your paper, the following queries arose. Please respond to these by marking up your proofs with the necessary changes/additions. Please write your answers on the query sheet if there is insufficient space on the page proofs. Please write clearly and follow the conventions shown on the attached corrections sheet. If returning the proof by fax do not write too close to the paper's edge. Please remember that illegible mark-ups may delay publication.

Many thanks for your assistance.

Query reference	Query	Remarks
1	AUTHOR: Please provide city, state, and country for reference 'Burbine 2000'.	
2	AUTHOR: Please provide page range for reference Burns 1970, if applicable.	
3	AUTHOR: Papers that have not yet been accepted for publication should not be included in the Reference List; they should be cited in the text as 'A. Author, unpublished data'. Please update Reference 'E. A. Cloutis et al.' if it has now been published, use 'in press' if it has been accepted for publication.	
4	AUTHOR: Please provide page range for reference Lane et al. 2009, if applicable.	
5	AUTHOR: Please provide the name of the publisher and city location of the publisher for Reference Mittlefehldt et al. 1998, if applicable.	
6	WILEY-BLACKWELL: Please provide more details (document title and all author names) for reference Morrow et al.	
7	WILEY-BLACKWELL: Please provide more details (document title and all author names) for reference Zolensky et al.	

Proof Correction Marks

Please correct and return your proofs using the proof correction marks below. For a more detailed look at using these marks please reference the most recent edition of The Chicago Manual of Style and visit them on the Web at: <http://www.chicagomanualofstyle.org/home.html>

<i>Instruction to typesetter</i>	<i>Textual mark</i>	<i>Marginal mark</i>
Leave unchanged	... under matter to remain	<u>stet</u>
Insert in text the matter indicated in the margin	^	^ followed by new matter
Delete	Ʒ through single character, rule or underline or Ʒ through all characters to be deleted	Ʒ
Substitute character or substitute part of one or more word(s)	Ƶ through letter or —— through characters	new character Ƶ or new characters Ƶ
Change to italics	— under matter to be changed	<u>ital</u>
Change to capitals	≡≡ under matter to be changed	<u>Caps</u>
Change to small capitals	≡≡ under matter to be changed	<u>sc</u>
Change to bold type	~ under matter to be changed	<u>bf</u>
Change to bold italic	~ under matter to be changed	<u>bf+ital</u>
Change to lower case	Ɔ	<u>lc</u>
Insert superscript	∨	∨ under character e.g. ∨
Insert subscript	^	^ over character e.g. ^
Insert full stop	⊙	⊙
Insert comma	↵	↵
Insert single quotation marks	↵ ↵	↵ ↵
Insert double quotation marks	↵ ↵	↵ ↵
Insert hyphen	=	=
Start new paragraph	¶	¶
Transpose	┌┐	┌┐
Close up	linking ○ characters	○
Insert or substitute space between characters or words	#	#
Reduce space between characters or words	◌	◌